

**SKB P-25-02**

ISSN 1651-4416

ID 2066034

May 2025

## **Forsmark site investigation**

### **Overcoring rock stress measurements in borehole KFM24**

Daniel Ask  
FracSinus Rock Stress Measurements AB

*Keywords:* Stress measurement, Three-dimensional overcoring, Borre Probe III, Stress state

This report concerns a study which was conducted for Svensk Kärnbränslehantering AB (SKB). The conclusions and viewpoints presented in the report are those of the author. SKB may draw modified conclusions, based on additional literature sources and/or expert opinions.

Data in SKB's database can be changed for different reasons. Minor changes in SKB's database will not necessarily result in a revised report. Data revisions may also be presented as supplements, available at [www.skb.se](http://www.skb.se).

This report is published on [www.skb.se](http://www.skb.se)

© 2025 Svensk Kärnbränslehantering AB

## Summary

Overcoring rock stress measurements with wireline technique and the *Borre Probe III* cell have been carried out in borehole KFM24, Forsmark. In total, four installations were made, of which three provided useful data. These measurements constitute the deepest tests executed in a surface drilled borehole with overcoring technique in Sweden.

Prior to the initiation of the overcoring measurement campaign, significant time and effort had to be spent cleaning the borehole from drill cuttings. Initial cleaning attempts by other parties were not sufficient for a successful overcoring campaign, where strain gauges are to be glued at the very bottom of the borehole. However, new cleaning attempts using high-capacity pump trucks were successful. Combined with the highly effective mammoth pump system of SKB, the stress measurement campaign could be undertaken according to plan.

The results indicate that the stress field in borehole KFM24 is dominated by a major principal stress that is horizontal. The intermediate and minor principal stress magnitudes are of the same order of magnitude meaning that their orientation cannot be resolved with precision. However, previously conducted hydraulic fracturing measurements in multiple boreholes at the Forsmark site have demonstrated that the vertical direction is aligned with a principal stress. Hence, this information was used to guide the stress calculations of the overcoring data. The guided solution is judged the most reliable and yields the following:

Length/Depth [mbl/mvd]	Magnitude [MPa]			Direction [°N]			Dip [°]		
	$\sigma_1=$	$\sigma_2=$	$\sigma_3=$	$\sigma_1=$	$\sigma_2=$	$\sigma_3=$	$\sigma_1=$	$\sigma_2=$	$\sigma_3=$
	$\sigma_H$	$\sigma_h$	$\sigma_v$	$\sigma_H$	$\sigma_h$	$\sigma_v$	$\sigma_H$	$\sigma_h$	$\sigma_v$
564.16/561.26	24.2	14.8	14.6	121	211	302	0	0	90

## Sammanfattning

Bergspänningsmätningar med överborrningsteknik har utförts i borrhål KFM24, Forsmark. Mätningarna utfördes med wirelineteknik och med cellen *Borre Probe III*. Totalt gjordes fyra installationer, varav tre resulterade i användbara data. Dessa mätningar utgör de djupaste proven utförda i ett ytborrat borrhål med överborrningsteknik i Sverige.

Innan mätningarna kunde påbörjas utfördes en omfattande renspolning av borrhålet från borrkax eftersom inledande rensningsförsök från andra parter inte var tillräckliga för de höga krav som ställs för överborrningsmätning. Renspolningsförsök av borrhålet med spolbil var lyckosamma och kax från de förnyade borringar som utfördes i samband med aktuell mätkampanj kunde elimineras med SKB:s mammutpumpsystem.

Resultaten indikerar att spänningsfältet i borrhål KFM24 domineras av en större huvudspänning som är horisontell. Den intermediära och den minsta huvudspänningen är av samma storleksordning, vilket innebär att deras orientering inte kan lösas med precision. Tidigare genomförda hydrauliska spänningsmätningar i flera borrhål i Forsmark har dock påvisat att en huvudspänning är vertikal. Denna information användes för att styra spänningsberäkningarna och anger följande slutresultat:

Längd/Djup [mbl/mvd]	Magnitud [MPa]			Riktning [°N]			Stupning [°]		
	$\sigma_1=$	$\sigma_2=$	$\sigma_3=$	$\sigma_1=$	$\sigma_2=$	$\sigma_3=$	$\sigma_1=$	$\sigma_2=$	$\sigma_3=$
	$\sigma_H$	$\sigma_h$	$\sigma_v$	$\sigma_H$	$\sigma_h$	$\sigma_v$	$\sigma_H$	$\sigma_h$	$\sigma_v$
564.16/561.26	24.2	14.8	14.6	121	211	302	0	0	90

# Content

<b>1</b>	<b>Introduction .....</b>	<b>4</b>
1.1	Purpose .....	4
1.2	Significant project deviation .....	5
1.3	Crew .....	6
<b>2</b>	<b>Measurement methodology with <i>Borre Probe III</i> .....</b>	<b>7</b>
2.1	General .....	7
2.2	Drilling technique.....	8
2.3	New developments of measurement technique .....	8
2.4	Theory .....	11
<b>3</b>	<b>Results .....</b>	<b>14</b>
3.1	Installation attempts .....	14
<b>4</b>	<b>Interpretation .....</b>	<b>18</b>
4.1	Calculation of elastic parameters.....	18
4.2	Stress calculations .....	20
4.2.1	Single measurement points and integrated solution .....	20
4.2.2	Guided stress calculations .....	20
<b>5</b>	<b>Discussion and conclusion.....</b>	<b>22</b>
	<b>References .....</b>	<b>24</b>
	<b>Appendix 1 – Pilot hole drilling and installations.....</b>	<b>25</b>
	<b>Appendix 2 – Biaxial test curves .....</b>	<b>32</b>
	<b>Appendix 3 – Overcoring strain curves.....</b>	<b>34</b>
	<b>Appendix 4 – Data used for stress calculation .....</b>	<b>39</b>

# 1 Introduction

## 1.1 Purpose

This report presents the results of the rock stress measurements in borehole KFM24 at Forsmark that SKB commissioned for FracSinus Rock Stress Measurements AB (hereafter referred to as FracSinus). The field work was undertaken between December 2<sup>nd</sup>, year 2024 and February 4<sup>th</sup>, year 2025. The goal for the project was to carry out three discrete measurements with *Borre Probe III* at approx. 560 m borehole length.

The measurement campaign was the third assignment by FracSinus related to overcoring stress measurements in the borehole KFM24 (Figure 1-1). In April 2021, two overcore samples were drilled to establish if the samples could be drilled without inducement of microfractures, a significant problem in previous overcoring measurements during the site investigation program (PLU; Hakami and Holmgren, 2021). The trial proved successful but no attempts to install measurement cells were undertaken.

In September year 2023, overcoring stress measurements were attempted using *Borre Probe III*. The campaign was terminated when it was clear that the borehole was contaminated by large amounts of drill cuttings, effectively preventing gluing of strain gauges in the bottom of the borehole.

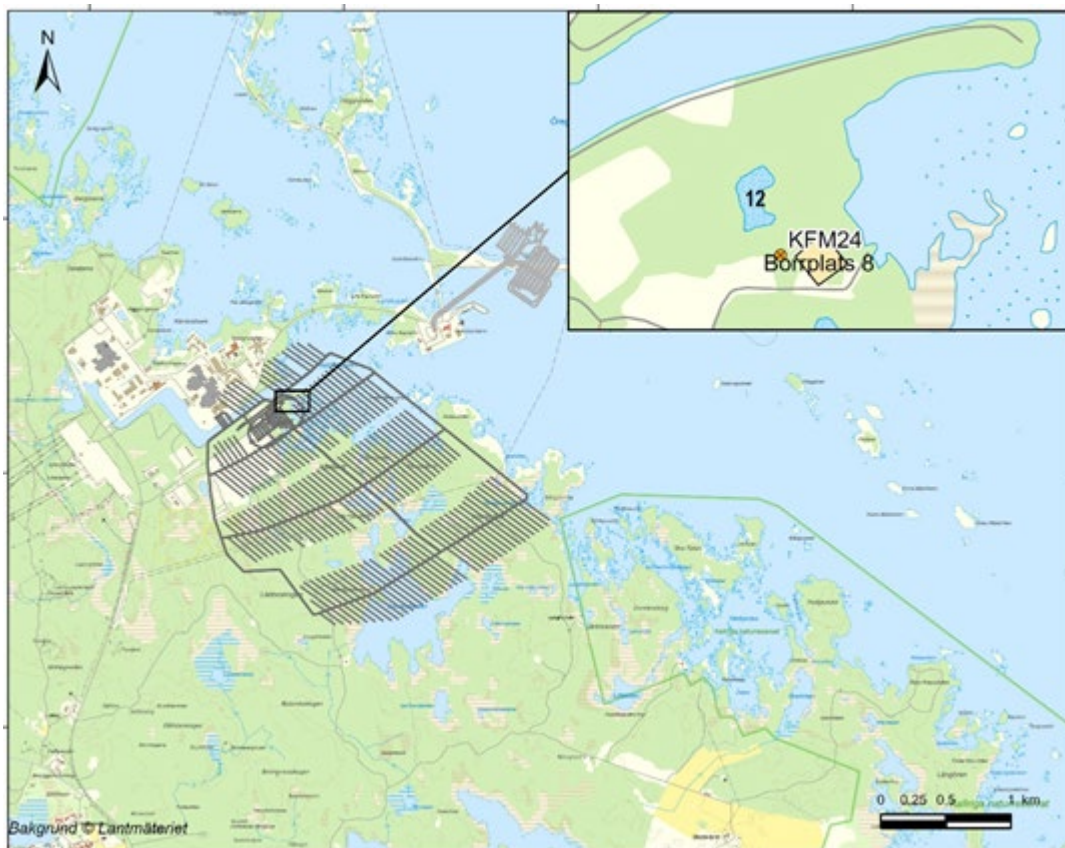


Figure 1-1. Location of borehole KFM24.

In the present project, emphasis was focusing on minimizing effects of drill cuttings in the borehole. Prior to project start, cleaning attempts were made by using nitrogen gas, and also a mammoth pump was installed. In addition, a specialized measurement equipment was developed allowing continuous pumping in the borehole in the stages just prior to cell installation. With these additional steps, it was judged that cleaning could be sufficient for overcoring stress measurements to be successful.

Results and data from reported activity are stored in the primary database Sicada, where they are traceable by the Activity Plan. The activities were conducted in compliance with the SKB internal controlling documents, activity plan, AP SFK-24-048, and SKB method description for rock stress measurement with the overcoring method, SKB MD 181.001e version 2.

## 1.2 Significant project deviation

Initially, it was estimated that one measurement could be completed during one working week of four days. As the goal was to conduct three measurement points, the aim was to complete all measurements prior to the Christmas holiday of 2024. Regrettably, it was immediately clear that the cleaning operations using nitrogen gas and mammoth pumping system prior to site establishment had not been sufficient enough in relation to the large amounts of drill cutting debris present in the borehole (Figure 1-2).

Despite very extensive flushing, it was not possible to clean the borehole to a satisfactory level. In addition, only one of the two pipes to the mammoth system was functioning, reducing the pump efficiency. Attempts to flush the NQ-sized borehole with nitrogen gas were undertaken but the pressure in the gas cylinders was too low to penetrate to full borehole depth. Furthermore, the gas leakage in the drill string was fairly substantial, limiting the cleaning effect.

It was now proposed to attempt to flush the NQ-sized borehole using a pump truck with a flow and pressure capacity much exceeding that of the flushing equipment available at the site. The action was approved by SKB and the NQ-sized borehole was flushed using a flow of about 400 l/min with a total of 16 m<sup>3</sup> of fluorescent Uranine marked water from SKB's approved water post. Surprisingly, not even this did completely resolve the drill cuttings issue, and the borehole cameras of FracSinus were brought to site to shed some light on the problem. Filming indicated that the remaining culprit was a mud cake behind the previous position of the cone in the intersection between the slim and large diameter parts of the borehole (Figure 1-3). However, filming also demonstrated that the NQ-sized borehole was now satisfactorily clean. It was again decided to use a pump truck to clean the large diameter borehole, but for this to be effective, the mammoth pump system and the inner casing must be hoisted. Once lifted, it was clear that the mud cake had plugged one of the pipes of the mammoth pump.



*Figure 1-2. Water sample taken before and after the cleaning operations in borehole KFM24.*



*Figure 1-3. Mud cake visible on the cone, placed in the intersection between the slim and large diameter parts of the borehole. Based on the traces along the cone assembly, a mud cake extending at least 2.1 m above the bottom plate was clearly visible.*

Prior to cleaning the upper large diameter part of the borehole, a plug was manufactured to prevent that debris would fall into the cleaned NQ-sized borehole during the operation. The subsequent cleaning of the large diameter part of the borehole was finally successful and the result was verified using the borehole cameras of FracSinus.

The cleaning operations and the extensive flushing during the overcoring measurement campaign resulted in a staggering consumption of water. In total, about 161 m<sup>3</sup> of Uranine stained water has been pumped into the borehole. During the water injection into the borehole, much of the water returned up the borehole and discharged on the ground surface. However, the volume of water reverted to the surface is difficult to estimate, and hence also the volume injected into rock fractures. This is important to consider if subsequent chemical investigations are to be made.

Conclusively, the cleaning operations were successful, but the entire length of the planned measurement campaign had at that time been used and measurements attempts were not initiated until after the Christmas holidays. In January-February of 2025, four installation attempts were made during 4 weeks, i.e. precisely according to the estimated time requirement per overcoring test.

### **1.3 Crew**

The tool development (section 2.3), based on drawings of FracSinus, was undertaken at the Central Workshop of Luleå University of Technology. The work was led by Daniel Ask and manufacturing was primarily undertaken by Tommy Nilsson, FracSinus/LTU, with assistance from Fredrik Nilsson and Mats Lindfors, both LTU.

The measurement attempts were carried out by Daniel Ask, FracSinus, in collaboration with Jan-Arvid Pettersson and Jonny Skagerstam, Drillcon Scandinavia AB.

## 2 Measurement methodology with *Borre Probe III*

### 2.1 General

The overcoring method is based on the fact that the *in situ* stresses can be calculated from the deformations that occur in the drill core while relieved during overcoring. The *in situ* stresses can be calculated from measured strains and with knowledge of the rock's elastic parameters. The complete three-dimensional stress tensor can be determined in a single measurement, under the assumption that the rock is continuous, homogeneous, and isotropic, as well as behaving linear-elastically (Leeman and Hayes, 1966; Leeman, 1968).

The *Borre Probe* was first developed by Vattenfall and then further improved by SwedPower AB, Vattenfall Power Consultant AB, Pöyry SwedPower AB, Geosigma AB and finally FracSinus RSM AB. The technical details regarding equipment and method have been presented by Sjöberg and Klasson (2003), and no further description is given here.

For a complete determination of the three-dimensional state of stress, measurement in six mutually independent directions is required. Field data from an overcoring measurement with the *Borre Probe III* measuring cell consists of nine (9) strain differences in seven (7) independent directions, as a result of that the drill core, in which the strain sensors are glued, is being cut off from surrounding rock pressure in connection with the overcoring. This means a slight redundancy in the data that enables the performance of a linear regression analysis to find the solution that best fits all measured strains. The measurement method implies that each successful measurement allows a complete stress calculation in three dimensions. The repetition of the measurement procedure in several points at the same level/depth in a borehole aims to increase the reliability of the results. The dispersions obtained will give an indication of uncertainties in the measurement data.

*Borre Probe*, version III, was modernized in 2003 and equipped with a new data logger (SwedPower AB). This new data logger enables strain registration both during gluing and during the overcoring process. Through gluing, registration is done every 15 minutes and during overcoring, the measurement interval can be selected between 3 and 60 s. Normally, strain registration is selected every 3 seconds.

After overcoring of the measuring cell, supplementary determinations of the rock's elastic parameters – modulus of elasticity,  $E$ , and Poisson's ratio,  $\nu$ , – are carried out by pressurizing the rock core in a so-called biaxial cell. The overcore is subjected to a successively increasing external, enveloping overpressure up to 10 MPa, then a successively decreasing pressure, in pressure increments of 1 MPa. This procedure is performed immediately after retrieving the drill core.

Evaluation of the stresses is based on the strain differences, determined as the difference in strain value before and after free drilling of the measuring cell, as well as the values of the elastic parameters of the rock sample. Calculations of stresses from measured strains are based on the classical theory of Leeman (1968) and are computerized. A more detailed theoretical description of the methodology is given in Chapter 2.2.

Briefly, the stress calculation is done so that a computer program determines the magnitude and orientation of the principal stresses ( $\sigma_1$ ,  $\sigma_2$ , and  $\sigma_3$ ) based on strain differences and measured material parameters for each measurement point. These vector quantities are then projected (and recalculated) onto the horizontal and vertical plane, whereby the horizontal and vertical stresses ( $\sigma_H$ ,  $\sigma_h$ , and  $\sigma_v$ ) are obtained. Averaging the results from several measurement points takes place in the main stress plane, which gives a so-called average value plane for the main stresses. In order to obtain average values of horizontal and vertical stresses, this average value plane for the principal stresses is projected (and recalculated) to the horizontal and vertical planes.

The method requires that approx. 25 cm of the pilot hole for installation of the measuring cell is fracture free. The minimum length for the core to fill the biaxial chamber is 21-25 cm (depending on overcore dimension). Apart from the fact that fractures must not exist, it is important that the grain size is homogeneous, as the theory is based on the assumption of linear elastic conditions. For example, "core dinking" makes stress measurement with overcoring impossible in practice (or makes the measurement results extremely uncertain). It is therefore possible that several pilot holes have to be drilled before finding an acceptable location for measurement/installation.

The method is relatively sensitive to the appearance of microcracks in the overcore sample, especially in smaller overcoring dimension (76 mm). If high stresses are expected, one should, if possible, avoid orienting the borehole perpendicular to the expected direction of the greatest principal stress and increase the overcoring dimension. Finally, it is of the utmost importance that the pilot hole wall is completely clean, as the strain rosettes must be glued, i.e. there must not be any kind of coating (e.g. chemical depositions) or drill cuttings in the pilot hole.

For the evaluation, it is also assumed that the rock sample can be described as continuous, homogeneous, isotropic and behaves linearly elastically. In addition to the known theoretical relationships, some visual assessment of the measurement results is required to check the function of individual strain gauges.

## 2.2 Drilling technique

The *Borre Probe III* cell can be installed in arbitrarily oriented boreholes. The boreholes to be installed can be dry or water-filled, and measurements can be made at great borehole depths (borehole length record is 640 m in Finland). In horizontal and upwards oriented boreholes, fiberglass rods are commonly used to insert the cell into the pilot hole, which limits the borehole length to about 50 m.

Dimension of the borehole, and thus the wall thickness of the overcored rock cylinder, is controlled by the assessed stress situation. The most common dimension for *Borre Probe III* is  $\varnothing 76$  mm, enabling both conventional drilling and wireline technology. For larger borehole dimensions, such as  $\varnothing 116$ ,  $\varnothing 131$  and  $\varnothing 146$  mm, drilling is possible to be performed only using conventional technology.

Since the overcoring technique includes several drilling phases, there is a significant time, and thus financial, advantage by applying wireline technique. This advantage also becomes exponentially more important with increasing hole length.

The wireline system of FracSinus for NQ holes is based on Atlas Copco's CORAC system, which can surface mill the borehole bottom, pilot drill, and flush the pilot hole with the string remaining in the borehole. If the rock is of poor quality, the pilot is drilled out and the procedure is repeated. This means that the string can remain in the borehole until a pilot core is accepted for installation.

However, the installation of the measuring cell itself requires an open borehole and the overcoring uses a thin-walled core tube (Atlas Copco T2-76) in order for the cell wall in the rock sample to be large enough to avoid microcracks. Thus, raising and lowering of the string is required at each installation of the measuring cell.

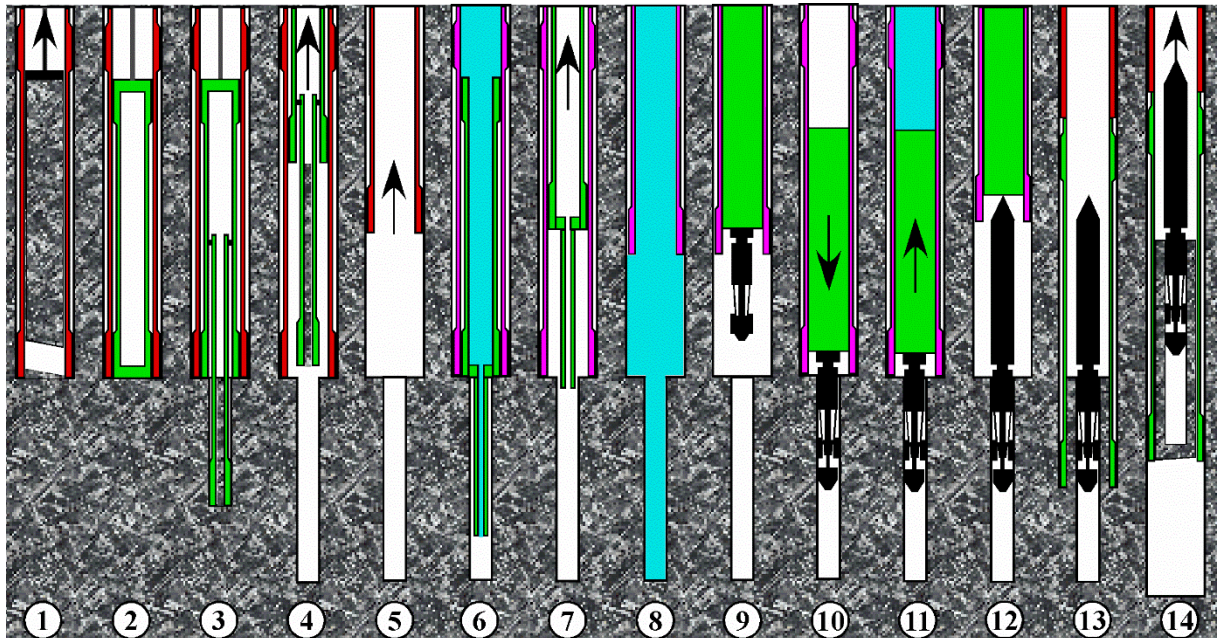
## 2.3 New developments of measurement technique

In the previous overcoring attempts in borehole KFM24, it was demonstrated that the wire-line equipment of FracSinus could grind the borehole bottom, drill centralized pilot holes, and overcore the rock samples without any tendency of ring discing. This was even possible with the CORAC core barrel, which yields a wall thickness of only around 5 mm. However, at the project start for overcoring measurements in borehole KFM24, the rock cylinders were completely filled with drill cuttings and hence the campaign was forced to be terminated without any installation attempts.

To flush out already existing drill cuttings and to minimize sedimentation in the borehole of cuttings during the continued drilling operations, continuous mammoth pumping was undertaken during the entire duration of the project. This pump system effectively ensured that cuttings were flushed out of the large diameter section within the top 37 m of the borehole.

Specific for this project, a new wireline operated insert for cell installation was developed in order to diminish the negative effects of drill cuttings, as well as to reduce the risks for measurements at great borehole lengths. With this insert, the cell can be installed with the drill string remaining in the borehole, thus eliminating the somewhat risky conventional open hole installation; a risk much augmented with increasing depth. Simultaneously, with this insert, almost continuous pumping in the string could be performed, thereby further reducing the risk of sedimentation of drill cuttings. In this respect, it should be noted that the measurement now performed in borehole KFM24 at Forsmark corresponds to the longest borehole length so far attempted in Sweden using overcoring technique.

To facilitate the modification, the drill bit of the CORAC core barrel must be exchanged as the inner diameter of the bit is only about 47 mm – too small for *Borre Probe III*-cell to pass. Once exchanged with a core bit adapter, the CORAC barrel can be lowered together with the flushing insert (see Figure 2-1, Figure 2-2, and Figure 2-3).



1. Borehole,  $\phi 76$  mm, is flushed after drilling
2. Grinding of the borehole bottom with full face bit.
3. Pilot hole,  $\phi 36$  mm, is drilled.
4. Pilot hole core is hoisted for inspection. If the position is deemed non-suitable for installation, the pilot is removed and the process restarts at step 1.
5. If the position is accepted for installation, the drill string is lifted for adjustment of the CORAC core barrel (removal of the drill bit with an adapter).
6. Lowering of the modified CORAC core barrel together with the wire-line flushing insert and flushing of pilot hole.
7. Hoisting of wire-line flushing tool – this is now the only step where some back-flow may occur.
8. Once hoisted, pumping into the string is restarted while the wire-line cell installation insert is prepared.
9. The measurement cell and the orientation unit is programmed and then installed in the wire-line insert. The insert is carefully lowered and locks in position in the core barrel similar to other inserts. Verification of successful lowering and latching of the insert in the core barrel is controlled by that a small force is required to break a pin to retrieve the wire-line spear.
10. Installation of the cell is made by lowering the drill string to the bottom of the borehole and by letting it rest there. During this step, another breaker pin is activated and releases the *Borre Probe III*-cell from the insert. From this stage and forward, the cell is no longer sensitive to sedimentation of any remaining drill cuttings. Glue hardening phase now takes place (8-12 h), normally over the night, and the wire-line spear can be hoisted to surface.
11. After the glue hardening phase, the drill string is pressurized to 3 bars and the string is carefully hoisted. Successful release of the cell is indicated by a pressure drop and the string can thereafter be hoisted normally. Once the cell is stand-alone in the borehole, the orientation device will give proper values for verification of cell orientation downhole.
12. Descent with T2-76 core barrel.
13. Overcoring and release of stress field.
14. Core break and hoisting of cell and overcore sample to surface.

**Figure 2-1.** Modified overcoring methodology with the *Borre Probe III*-cell.

Flushing is conducted until the borehole is completely clean and the flushing insert can then be hoisted to surface. As this hoisting may cause some back-flow, it is undertaken with reduced speed. Once the flushing tool has been retrieved, pumping in the open string can be initiated once more, while the cell installation insert is prepared, preventing any remaining cuttings to descend towards the bottom of the borehole.

The cell installation insert is thereafter lowered in the string using the wireline, whereby the descent can be fully controlled. Once at the bottom of the drill string, it is possible to control that the insert has latched correctly in the core barrel as a pin must be broken to retrieve the wireline spear used for descent. Having established that the insert is in the correct position, the installation of the measurement cell in the pilot hole is completed by a careful descent of the string and by letting it rest at the borehole bottom.

To release the cell from the string, the string is firstly pressurized to 3 bars, and thereafter hoisted slowly until a pressure drop is visible. This pressure drop indicates that the cell is free-standing and fully released from the string and installation insert. The string can then be hoisted normally. Thereafter the cell is left for glue hardening over night.

Overcoring is made using a T2-76 core barrel, requiring a round-trip with the string similar to the conventional installation methodology.

It should be noted that the combination of the CORAC and T2-76 core barrels has some implications, apart from the core size difference, as they produce also a slight difference in borehole diameters. CORAC is a NQ system, giving a borehole diameter of 75.7 mm, whereas the T2-76 barrel is a metric system producing a borehole diameter of 76.0 mm. Generally, in order to minimize drilling problems, new reaming shells are used on the CORAC core barrel and worn down reaming shells are used on the T2-76 core barrel, to minimize this difference. Yet, there is often a small edge in the borehole, about 10 cm above the borehole bottom (the length of the CORAC drill bit ahead of the reaming shell) that offers some resistance when drilling with T2-76. For short boreholes, when length precision is excellent, this is easily recognizable but for longer borehole, this is much more difficult, as the string suffers from a degree of compliance and flexibility.



**Figure 2-2.** Left: Front section of CORAC core barrel inserts. Cell installation insert in the top, the borehole grinding and pilot hole drilling insert in the middle, and the flushing tool insert at the bottom. Right: This image displays the original Borre Probe III cell (right) and the modified cell (left), with front ring on rosette holder, new external pipe, and a new bronze top with breaker pin, internal orientation device and external o-ring seal. The latter functions as a control measure during the release of the cell after installation, providing a clear indication of pressure drop in the pressurized string when the string is hoisted.



**Figure 2-3.** Left: Drill bit adapter for the CORAC core barrel. Right: The lowering tool for the installation insert. Once the installation insert has latched in the core barrel, the retrieval of the lowering tool requires pulling off a breaker pin, thus providing an indication that the installation insert is correctly installed in the core barrel.

To reduce risk for error, the overcoring procedure is altered slightly as compared to short boreholes. For deep boreholes, the T2-76 barrel is halted some 50 cm above the borehole bottom, instead of just above the bottom. The implications of this modification is that the start of flushing and start of string rotation prior to overcoring is not clearly visible on the strain versus time plots.

Conclusively, the new installation methodology requires one more round-trip with the string. This is of course unfortunate, but it is judged as a very reasonable cost spending on the tremendous risk reduction achieved, and the ability to ensure almost constant flushing of the borehole to remove drill cuttings.

## 2.4 Theory

The overcoring method is generally based on the assumption that the rock is linear elastic and isotropic, although interpretation methods for anisotropic conditions have been developed (Amadei and Stephansson, 1997). The deformation of the drill core during overcoring is assumed to be identical in magnitude to the deformation resulting from the unloading the stress field, but with different signs. Application of elasticity theory also means that the material properties of the rock must be known, i.e. modulus of elasticity ( $E$ , Young's modulus) and transverse contraction ratio ( $\nu$ , Poisson's ratio). The rock is further assumed to be continuous and homogeneous and that the cell is mounted at a sufficiently large distance from the ends of the borehole so that end effects can be neglected (Merril, 1964; Amadei and Stephansson, 1997).

For *Borre Probe III*, only the rosettes are glued onto the rock and no correction factors are necessary (a so-called CSIR-type cell). In addition, glue specially developed for the *Borre Probe* cell is used, i.e. a glue that is recognized to be very stable and with extremely little drift over time.

Under these conditions, the deformations around the borehole can be described according to Hirashima and Koga (1977):

$$u_r = \frac{1+\nu}{2E} r \left[ \frac{R^2}{r^2} (\sigma_x + \sigma_y) + \left\{ 1 + 4(1-\nu) \frac{R^2}{r^2} - \frac{R^4}{r^4} \right\} \{ (\sigma_x - \sigma_y) \cos 2\theta + 2\tau_{xy} \sin 2\theta \} \right. \\ \left. + \left\{ \frac{1-\nu}{1+\nu} (\sigma_x + \sigma_y) - 2 \frac{\nu}{1+\nu} \sigma_z \right\} \right] \quad \text{Eq (1)}$$

$$u_\theta = -\frac{1+\nu}{2E} r \left[ \left\{ 1 + 2(1-2\nu) \frac{R^2}{r^2} + \frac{R^4}{r^4} \right\} \{ (\sigma_x - \sigma_y) \sin 2\theta - 2\tau_{xy} \cos 2\theta \} \right] \quad \text{Eq (2)}$$

$$u_z = \frac{1+\nu}{E} \left[ 2r \left( 1 + \frac{R^2}{r^2} \right) (\tau_{yz} \sin \theta + \tau_{zx} \cos \theta) + \frac{z}{1+\nu} \{ \sigma_z - \nu(\sigma_x + \sigma_y) \} \right] \quad \text{Eq (3)}$$

where R is the radius of the borehole, r is the radial distance to the measurement point, E and  $\nu$  are the modulus of elasticity and the transverse contraction number, z is the length in the direction of the borehole, and  $\theta$  is the position of the strain gauge in the borehole according to the selected coordinate system (xyz, see Figure 2-4). *Borre Probe III* has strain gauges oriented in axial, tangential, and 45° directions relative to the axis of the borehole. For these orientations, one obtains:

$$\varepsilon_{\theta} = \frac{1}{R} \left\{ (u_r)_{r=R} + \left( \frac{\partial u_{\theta}}{\partial \theta} \right)_{r=R} \right\} \quad \text{Eq (4)}$$

$$\varepsilon_z = \left( \frac{\partial u_z}{\partial z} \right)_{r=R} \quad \text{Eq (5)}$$

$$\gamma_{\theta z} = \frac{1}{R} \left( \frac{\partial u_z}{\partial \theta} \right)_{r=R} \quad \text{Eq (6)}$$

$$\varepsilon_{45^\circ} = \frac{1}{2} (\varepsilon_{\theta} + \varepsilon_z + \gamma_{\theta z}) \quad \text{Eq (7)}$$

where

$$\left( \frac{\partial u_{\theta}}{\partial \theta} \right)_{r=R} = -\frac{4(1-\nu^2)}{E} R [(\sigma_x - \sigma_y) \cos 2\theta + 2\tau_{xy} \sin 2\theta] \quad \text{Eq (8)}$$

$$\left( \frac{\partial u_z}{\partial z} \right)_{r=R} = \frac{1}{E} [\sigma_z - \nu(\sigma_x + \sigma_y)] \quad \text{Eq (9)}$$

$$\left( \frac{\partial u_z}{\partial \theta} \right)_{r=R} = \frac{R}{E} [4(1+\nu)(\tau_{yz} \cos \theta - \tau_{zx} \sin \theta)] \quad \text{Eq (10)}$$

Combining equations 4 to 10 and setting  $r = R$  gives the final solution:

$$\varepsilon_{\theta} = [(\sigma_x + \sigma_y) - 2(1-\nu^2)\{(\sigma_x - \sigma_y) \cos 2\theta + 2\tau_{xy} \sin 2\theta\} - \nu\sigma_z]/E \quad \text{Eq (11)}$$

$$\varepsilon_z = [\sigma_z - \nu(\sigma_x + \sigma_y)]/E \quad \text{Eq (12)}$$

$$\varepsilon_{\pm 45^\circ} = 0.5(\varepsilon_{\theta} + \varepsilon_z \pm 4(1+\nu)(\tau_{yz} \cos \theta - \tau_{zx} \sin \theta))/E \quad \text{Eq (13)}$$

The prevailing stress is derived through inversion methodology of measured strain data using proprietary data codes. The elastic parameters are derived by considering an infinitely long, thick-walled cylinder that is loaded with a homogeneous external load under the assumption that a plane state of stress prevails (Worotnicki, 1993; Amadei and Stephansson, 1997):

$$E = \frac{p}{\varepsilon_{\theta}} \frac{2}{1 - \left(\frac{D_i}{D_o}\right)^2} \quad \text{Eq (14)}$$

$$\nu = -\frac{\varepsilon_z}{\varepsilon_{\theta}} \quad \text{Eq (15)}$$

where p is load increment,  $\varepsilon_{\theta}$  and  $\varepsilon_z$  are the tangential and axial strain and  $D_i$  and  $D_o$  are the inner and outer diameter of the cylinder. If the number of gauges is few as a result of problems during the biaxial test, the gauges oriented at 45° angle can also be utilized according to (Ask, 2006):

$$E = \frac{p}{(2\varepsilon_{\pm 45} - \varepsilon_z)} \frac{2}{1 - \left(\frac{D_i}{D_o}\right)^2} \quad \text{Eq (16)}$$

$$\nu = -\frac{(2\varepsilon_{\pm 45} - \varepsilon_{\theta})}{(2\varepsilon_{\pm 45} - \varepsilon_z)} \quad \text{Eq (17)}$$

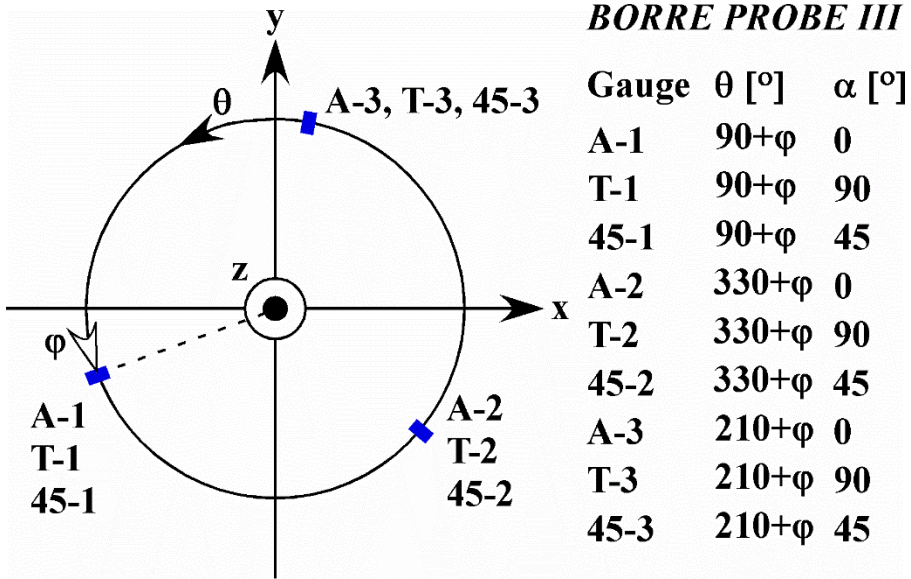


**Figure 2-4.** Coordinate system for Borre Probe III in the local system (the borehole). Cell orientation is arbitrary and is given by a rotation angle ( $\theta$ ) and the angle of the individual strain gauges relative to the borehole axis ( $\alpha$ ).

## 3 Results

In this chapter, a brief description of (a) the grinding of the borehole bottom, (b) the pilot hole drilling, (c) the installation attempt, (d) the overcoring process, (e) the biaxial testing, and (f) the gluing of the strain gauges are briefly described. The results are summarized in Table 3-1 and Table 3-2. More detailed information is presented in Appendices.

### 3.1 Installation attempts

#### *Installation 1:1:1*

- a) Grinding of borehole not perfect and resulted in a 9.5 mm central plateau. The likely cause is loss of o-rings at the top of the grinding/pilot hole inserts that prevented correct latching of the insert in the core barrel (Figure 3-1).  
The drill string was accidentally dropped a short distance down to the bottom of the borehole as a result of loss of fluid pressure in drill rig. After repair of the drill rig, the borehole bottom was re-grinded 12 cm, to remove potential damaged rock at the top of the pilot hole.
- b) Pilot hole drilling successful and pilot core accepted for installation.
- c) Installation failed as o-rings prevented correct installation of the strain gauges.
- d) No useful data obtained from the overcoring.
- e) Biaxial test not conducted.
- f) Orientation of strain rosettes is OK, but none of the gauges are glued onto the rock surface of the pilot hole.

#### *Installation 1:2:2*

- a) Grinding of the borehole bottom successful.
- b) Pilot hole drilling successful and pilot core accepted for installation.
- c) Installation only partly successful as o-rings prevented correct installation of the strain gauges. Only one rosette is glued properly and the cell is installed somewhat inclined to the overcore sample. Glue hardening of rosette 2 OK.
- d) Overcoring data from rosette 2 is successful with a very nice core break as we lift in a pre-existing fracture.
- e) Overcore sample fractures in the top of the sample during loading between 80 and 90 bar. Although not visible to the naked eye, a tensile microfracture developed during the overcoring as a result of that the cell was not perfectly aligned with the axis of the overcore sample (Figure 3-2).
- f) Orientation of strain rosettes is OK, but only rosette 2 is glued properly.



**Figure 3-1.** Top of CORAC wireline insert with latching piece, water tight seal, and radial lock moving from top and downwards on the photo. O-rings were lost and prevented proper installation for both test 1:1:1 and 1:2:2. Likely, these came off during dropping of the insert in the string, which is the normal procedure, but in KFM24 when using the mammoth pump, the water level was as far as 37 m down. The resulting force when hitting the water surface likely peeled off the o-rings. A change to stiffer o-rings and water filling of the borehole prior to dropping the inserts effectively remedied this problem.



**Figure 3-2.** In test 1:2:2, a number of lost o-rings got stuck on one side of the pilot hole resulting in a somewhat inclined installation of the cell (left). The top of the cell rested on the core barrel inner tube and during the overcoring process, this gave rise to tensile stress in the top part of the overcore sample. This entailed that a microfracture developed at the top of the overcore sample after a few minutes of drilling, that later propagated to a macrofracture during the subsequent biaxial test (right).

#### **Installation 1:3:3**

- a) Grinding of the borehole bottom successful.
- b) Pilot hole drilling successful and pilot core accepted for installation.
- c) Installation successful and glue hardening as expected.
- d) Overcoring data from all rosettes are very stable until core break, which was truly violent.
- e) Biaxial testing conducted in two steps, 0-7-0 and 0-10-0, but results are affected by the violent core break.
- f) Orientation of strain rosettes is successful and all gauges are very nicely bonded to the rock sample.

#### **Installation 1:4:4**

- a) Grinding of the borehole bottom successful.
- b) Pilot hole drilling successful and pilot core accepted for installation.
- c) Installation successful and glue hardening as expected.
- d) Overcoring data from all rosettes are very stable and core break is soft in pre-existing fracture. Yet, the overcore sample regrettably yields during the hoisting from depth up to surface.
- e) Biaxial testing conducted in two steps, 0-7-0 and 0-10-0, suffer from microfracturing.
- f) Orientation of strain rosettes is successful and all gauges are very nicely bonded to the rock sample.

**Table 3-1 Installation attempts in borehole KFM24.**

Measurement point	Grinding [mbl]	Pilot [mbl]	Overcoring [mbl]	Strain data, overcoring	Strain data, biaxial test
1:1:1	562.22-562.32 562.32-562.37 562.37-562.49	562.37-563.09	562.49-563.08	None	None
1:2:2	563.08-563.18	563.18-563.90	563.18-563.81	Rosette 2	Rosette 2
1:3:3	563.81-563.94 563.94-563.97	563.94-564.69	563.97-564.59	All rosettes	All rosettes
1:4:4	564.59-564.85 564.85-564.86	564.86-565.57	564.86-565.48	All rosettes	All rosettes

**Table 3-2 Pilot hole drilling and T2-76 overcore sample, borehole KFM24.**

Pilot	Outer diameter, pilot core [mm]	Inner diameter, T2-76 core [mm]	Outer diameter, T2-76 core [mm]	Pilot hole eccentricity	
				Start [mm]	End [mm]
1:1:1	21.7	36.5	61.5	0.05	0.25 at 55 cm length
1:2:2	21.7	36.5	61.5	0.35	1.15 at 62 cm length
1:3:3	21.7	36.5	61.5	0.15	0.15 at 56 cm length
1:4:4	21.7	36.3	61.5	0.20	0.35 at 66 cm length

## 4 Interpretation

In total, four installation attempts were conducted. The two first were not optimal as o-rings were lost, falling into the bottom of the borehole and preventing a correct installation of the strain gauges. Only one strain rosette from the first two measurement attempts provided data. Installations 3 and 4 were completely successful during the overcoring phases, but suffer from microfracturing during the biaxial test.

### 4.1 Calculation of elastic parameters

Biaxial tests should be undertaken to strain levels that are as close as possible to those observed during overcoring, generally 0-10-0 MPa with 1 MPa increment. For stress calculation, the unloading parameters are preferred as these mimic the situation during the overcoring procedure. Unloading parameters are evaluated as secant values between 3 MPa and 10 MPa. Observed weaknesses in the overcore sample may force a reduction of the pressure level. Generally, at least one overcore sample is subjected to two biaxial tests, to enable evaluation if the biaxial test itself may generate microfractures. All of the overcore tests were conducted on the common granite to granodiorite rock type 101057 in rock domain RFM029 and, in particular, showing a faint albitization alteration in the overcore samples.

In Test 1:2:2, the cell was installed somewhat inclined as o-rings disturbed the installation. As a result, the rock sample was subjected to a force perpendicular to the borehole axis during overcoring. A few minutes into the overcoring process, this force resulted in microfracturing within the top part of the core sample, which is clearly visible on the strain gauge response (Appendix 2 and 3). This microfracturing was not visible for the naked eye but resulted in a macrofracture during the biaxial testing. Consequently, the result from the strain rosette is somewhat uncertain and the pre-fracturing loading parameters are probably more realistic than the post-fracturing unloading parameters.

The core break after overcoring sample 1:3:3 was very violent and this generally causes damage of the overcore sample and potentially the glue bonding, leading to a reduced reliability of the biaxial test result. In Test 1:4:4, core break was successfully completed in a pre-existing fracture, leading to a soft and smooth core break. However, a few minutes after core break, the overcore sample shows clear signs of yielding. At these depths, involving almost 190 drill string pipes of 3 m length, the hoisting results in an unavoidable shaking of the overcore sample. Moreover, during this hoisting, each pipe requires a re-gripping of the pipe resulting in almost 380 distinct stops and restarts before the overcore sample reaches the surface. Naturally, drillers are extremely careful during this hoisting, but the hoisting is not always successful at very large depth, for which the drill string is compliant and behaves more like a giant spring rather than a stiff pipe. As a result, the biaxial test result are not optimal.

This outcome is very unfortunate as linearity, isotropy, and degree of hysteresis during the biaxial test are crucial for evaluating the validity of the inherent assumptions of the overcoring measurement technique. With obvious microfracturing of the overcore samples, such analysis becomes subjective (Table 4-1). However, it is clear that the hysteresis remains low for all gauges and seemingly independent of strain gauge orientation, i.e. all strains return to the initial value after completion of the biaxial test (except for Test 1:2:2 which fractured during biaxial testing). This implies that the cumulative microfracturing after overcoring and biaxial testing is fairly limited.

There is a degree of anisotropy, here evaluated at peak pressure (Table 4-1), but it hardly reaches levels that require analysis using anisotropic solutions (more than 30 %). A far more likely explanation for the observed spread between rosettes is the microfracturing of the overcore sample.

It may be concluded that the biaxial test results curves display smallest anisotropy for the strain gauges oriented parallel to the overcore sample. This is an important finding as it suggests that the observed microfracturing does not primarily involve fractures oriented perpendicular to the core axis. Such fractures were frequently observed during previous overcoring campaigns at the Forsmark site, often leading to ring discing phenomena.

The biaxial test results instead suggest microfracturing parallel and/or inclined to the core axis during the violent core break of Test 1:3:3 and during hoisting of Test 1:4:4. It is suggested that the observed microfracturing occurs along the lamination, which is sub-parallel to the core axis (Figure 4-1).

**Table 4-1 Hysteresis after completed biaxial test and anisotropy at peak load of biaxial test, borehole KFM24.**

Sample	Cycle [MPa]	Hysteresis [μstrain] (0/45/90)	Anisotropy [%] (R1/R2: R1/R3:R2/R3)	Comment
1:2:2	0-9-0	(14/57/16)	-	Only R2, core fractured
1:3:3a	0-7-0	(6/7/3)	(14:24:49)	
1:3:3b	0-10-0	(4/1/2)	(7:20:34)	
1:4:4	0-10-0	(3/2/5)	(10:18:9)	

The calculated elastic parameters display quite a bit of scatter, an unfortunate result when microfracturing takes place (Table 4-2). The rosette of test 1:2:2 fractured during loading, and loading values prior to failure are therefore judged more realistic. The two biaxial tests on overcore sample 1:3:3 indicate very similar results, whereas overcore sample 1:4:4 displays significantly lower stiffness. For stress calculations, Young's modulus of 71.7 GPa and Poisson's ration of 0.22 are used.



Overcore sample 1:2:2

Overcore sample 1:3:3

Overcore sample 1:4:4

**Figure 4-1.** Grain size distribution of overcore samples 1:2:2, 1:3:3, and 1:4:4 displaying a preferred direction of stiffer grains sub-parallel to the borehole axis. All samples correspond to rock type 101057 with faint albitization.

**Table 4-2 Results from analysis of biaxial test data in borehole KFM24; favored data in bold font. All overcore samples correspond to Rock Type 101057 with faint albitization.**

Measurement point	Cycle [MPa]	Loading				Unloading			
		E [GPa]	E <sub>std</sub> [GPa]	v [-]	v <sub>std</sub> [-]	E [GPa]	E <sub>std</sub> [GPa]	v [-]	v <sub>std</sub> [-]
1:2:2	0-9-0	<b>73.5</b>	<b>7.9</b>	<b>0.26</b>	<b>0.01</b>	76.4	1.2	0.24	0.01
1:3:3a	0-7-0	73.1	3.6	0.25	0.04	<b>71.3</b>	<b>2.7</b>	<b>0.23</b>	<b>0.03</b>
1:3:3b	0-10-0	72.2	2.2	0.24	0.03	<b>71.7</b>	<b>3.3</b>	<b>0.22</b>	<b>0.04</b>
1:4:4	0-10-0	63.5	1.7	0.23	0.04	61.4	2.3	0.20	0.05
<b>Best solution</b>		<b>72.9</b>	-	<b>0.25</b>	-	<b>71.7</b>	-	<b>0.22</b>	-

## 4.2 Stress calculations

### 4.2.1 Single measurement points and integrated solution

The results of the stress calculations are visualized in Table 4-3, Table 4-4, and Figure 4-2. Data used for the calculations are presented in Appendix 4.

No calculations are possible for Test 1:2:2 but Test 1:3:3 and 1:4:4 demonstrate a well defined stress field at about 560 m vertical depth. As a result, the integrated solution is very similar and is consistent with all 21 available strain gauges. In fact, only one strain gauge is identified by the Chauvenet's criterion, but the solution is not altered when the gauge is rejected. All calculations are based on a Young's modulus of 71.7 GPa and Poisson's ratio of 0.22.

Common for all solutions is a dominant major principal stress/maximum horizontal stress and intermediate and minor principal stresses of almost the same order of magnitude. For stress tensors, this implies that the orientation of  $\sigma_2$  and  $\sigma_3$  are poorly defined and only the orientation of  $\sigma_1$  is known with confidence. The solution suggests that  $\sigma_2$  and  $\sigma_3$  are significantly inclined.

**Table 4-3 Results of stress calculations, individual measurement points, principal stresses in borehole KFM24 (RT90-RHB70).**

Test	Length/Depth [mbl/mvd]	Magnitude [MPa]			Direction [°N]			Dip [°]		
		$\sigma_1$	$\sigma_2$	$\sigma_3$	$\sigma_1$	$\sigma_2$	$\sigma_3$	$\sigma_1$	$\sigma_2$	$\sigma_3$
1:2:2	563.32/560.43	-	-	-	-	-	-	-	-	-
1:3:3	564.13/561.23	22.6	14.5	13.9	121	213	21	5	25	64
1:4:4	565.02/562.12	26.3	19.0	12.0	121	214	29	2	52	38
INT	564.16/561.26	<b>24.1</b>	<b>15.3</b>	<b>13.9</b>	<b>121</b>	<b>215</b>	<b>25</b>	<b>5</b>	<b>39</b>	<b>50</b>

**Table 4-4 Results of stress calculations, individual measurement points, horizontal-/vertical stresses in borehole KFM24 (RT90-RHB70).**

Test	Length/Depth [mbl/mvd]	Magnitude [MPa]				Direction [°N]	
		$\sigma_H$	$\sigma_h$	$\sigma_v$	$\sigma_{v, theory}$	$\sigma_H$	$\sigma_h$
1:2:2	563.32/560.43	-	-	-	14.9	-	-
1:3:3	564.13/561.23	22.6	14.4	14.0	14.9	121	31
1:4:4	565.02/562.12	26.3	14.6	16.3	14.9	120	30
INT	564.16/561.26	24.1	14.7	14.6	14.9	121	31

### 4.2.2 Guided stress calculations

The inclinations of the intermediate and minor principal stresses are contradicted by hydraulic fracturing tests undertaken at the Forsmark site (Klee and Rummel, 2004, Ask et al. 2007) in several boreholes. These tests yielded axial fractures in sub-vertical boreholes, which is a clear statement that one principal stress is vertical. That the vertical direction is principal is further strengthened by temperature induced borehole breakouts (Ask et al. 2006, Ringgaard, 2007a, 2007b, Ask and Ask, 2007,). As a result, a new set of calculations were undertaken in which the stress field was forced to be horizontal/vertical. The results are presented in Table 4-5 and Figure 4-2. This leaves 4 parameters to be resolved, namely the three principal stress magnitudes and the direction of maximum principal stress. The guided, integrated result is consistent with 20 of 21 strain gauges.

**Table 4-5 Results of guided stress calculations, individual measurement points, principal stresses in borehole KFM24 (RT90-RHB70).**

Test	Length/Depth [mbl/mvd]	Magnitude [MPa]			Direction [°N]			Dip [°]		
		$\sigma_1$	$\sigma_2$	$\sigma_3$	$\sigma_1$	$\sigma_2$	$\sigma_3$	$\sigma_1$	$\sigma_2$	$\sigma_3$
1:2:2	563.32/560.43	-	-	-	-	-	-	-	-	-
1:3:3	564.13/561.23	22.8	14.3	14.2	120	30	-	0	0	90
1:4:4	565.02/562.12	25.6	14.8	14.1	124	-	34	0	90	0
INT	564.16/561.26	<b>24.2</b>	<b>14.8</b>	<b>14.6</b>	<b>121</b>	<b>31</b>	-	<b>0</b>	<b>0</b>	<b>90</b>

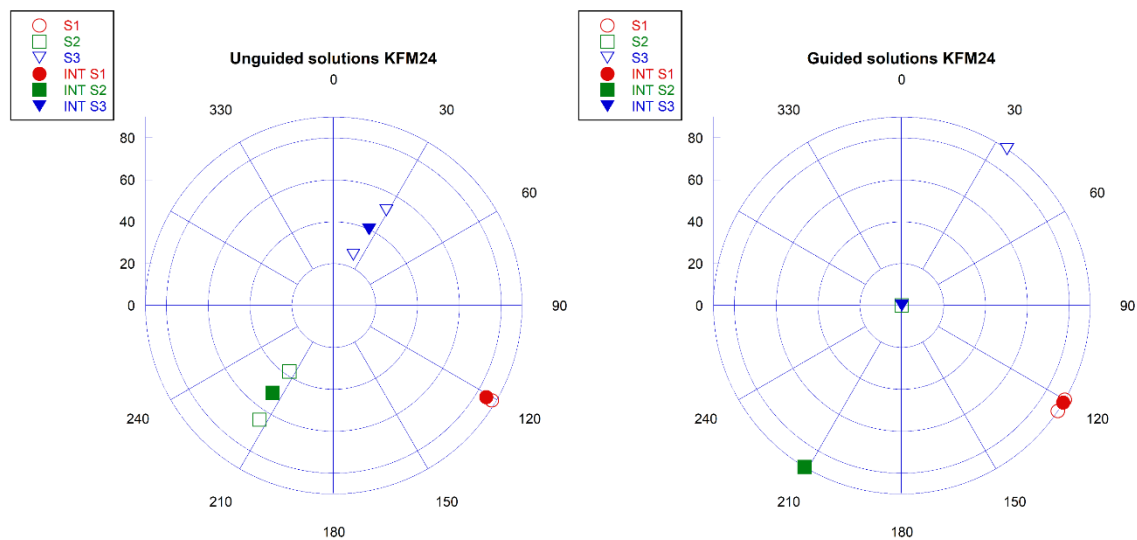


**Figure 4-2.** Lower hemisphere Schmidt projection of stress directions based on overcoring stress measurements in borehole KFM24; unguided (left) and guided solutions (right).

## 5 Discussion and conclusion

Stress measurements in borehole KFM24 proved to be a true challenge and only in this third attempt did the borehole finally reveal its secrets. The road was long and winding but obstacles could be resolved quite swiftly on the way.

Once the borehole was properly cleaned and the mammoth pump fully functioning, the flushing out of drill cuttings as the work progressed in the project was very effective. Yet, measurements at this depth means a flushing period of about 3-4 hours, i.e. a time consuming and thus a costly procedure. In addition, in the initial phase of the overcoring campaign, a series of o-rings on the wireline inserts were lost, but the problem could be identified and remedied.

The anticipated working schedule of one measurement per 4-day week could be upheld, but the work load for the drilling crew was substantial. Moreover, their work load shifted from very delicate, small dimension drilling to brute force during descent and hoisting of the string, which is not an ideal situation and requires a highly skilled drilling operator. It is clear that, although the new tool developments for this project worked without a single malfunction, it is not an optimal methodology to run deep overcoring stress measurements. Deep measurements should be made using a full wireline system, i.e. with the string left in the borehole at all times.

The results from the biaxial tests were not fully satisfactory, which is a drawback as these tests provide the elastic parameters used for stress calculation but also serve as a means to evaluate if the theoretical assumptions of the overcoring technique are fulfilled. The failure to provide unambiguous values of the elastic properties obviously reduces the reliability of the results.

The bedrock at the Forsmark site is rich in quartz, leading to a very high tensile strength. This is not optimal for core break after completed overcoring as it generally causes damage on the overcore sample and potentially also the glue bonding. The core break after overcoring Test 1:3:3 is best described as a downhole hand grenade making the whole drill rig jump. However, the gentle core break in a pre-existing fracture in Test 1:4:4 also resulted in yielding of the overcore sample, but this time during hoisting. Hoisting from these depths means lifting and locking the string twice on each 3 m pipe which has to be repeated 187 times before the core barrel can be reached. Each time, there is a ricochet along the string as it is nothing else than a giant spring at these borehole lengths. This resulted in tensile loads exceeding the strength of the overcore sample, which subsequently yielded. This indicates that overcoring using NQ/T2-76 size is just at the limit of what is possible at these depths in Forsmark. With a larger overcoring dimension, this could probably have been prevented.

In all three successful overcoring measurements, very stable strain responses are obtained and the exact timing of the failure of the overcoring samples can be readily identified; all occurring near the end (Test 1:2:2) and after the overcoring phase (Test 1:3:3 and 1:4:4). The overcoring strain response displays very stable strain values during overcoring and a very good repeatability between tests. Of the 21 strain gauges available, only one gauge was identified as an outlier based on Chauvenet's criterion for both the single measurement scale, and for the integrated solutions. As a result, data from the overcoring phase are judged very reliable.

The less optimal precision of the elastic parameters affects the final solution, but we still observe that the overcore samples show negligible hysteresis, moderate anisotropy, and sub-linear response, despite clear microfracturing. In addition, Young's modulus is high and Poisson's ratio low and in the same order of magnitude as those of controlled lab tests on solid cores ( $E=76$  GPa and  $\nu=0.24$  (Glamheden et al. 2007)). In addition, the calculated vertical stress in the solutions closely resembles the theoretical weight of the overburden rock mass. This implies that the values of the elastic parameters cannot be too far off, as this would affect the vertical stress component as well.

There is, however, one major restriction in the solution, namely that the intermediate and minor principal stress magnitudes are of a similar order of magnitude. This is a strictly mathematical limitation and means that the orientation of the  $\sigma_2/\sigma_3$ -plane is poorly defined and only the orientation of  $\sigma_1$  is known with confidence. The solution indicates that these principal stresses are strongly inclined, but they are in fact unresolved. To resolve this issue, guided stress calculations were undertaken forcing the stress field to be horizontal/vertical based on results from previous hydraulic fracturing stress measurements and temperature-induced, micro breakouts. These tests and observations demonstrated that one principal stress is indeed vertical at the Forsmark site. This guided solution of the prevailing stress field in borehole KFM24 is judged the most reliable.

## References

SKB's (Svensk Kärnbränslehantering AB) publications can be found at [www.skb.com/publications](http://www.skb.com/publications).

**Amadei B, Stephansson O, 1997.** Rock stress and its measurement. London: Chapman & Hall.

**Ask D, 2006.** New developments of the integrated stress determination method and application to the Äspö Hard Rock Laboratory. PhD Thesis, Royal Institute of Technology.

**Ask D, Ask M V S, 2007.** Forsmark site investigation. Detection of borehole breakouts in boreholes KFM01A and KFM01B. SKB P-07-235, Svensk Kärnbränslehantering AB.

**Ask M V S, Ask D, Christiansson R, 2006.** Detection of borehole breakouts at the Forsmark -site. In Proc. Int. Symp. On in-situ rock stress, (Trondheim, 2006), pp. 79-86.

**Ask D, Cornet F, Brunet C, Fontbonne F, 2007.** Forsmark site investigation. Stress measurements with hydraulic methods in boreholes KFM07A, KFM07C, KFM08A, KFM09A, and KFM09B. SKB P-07-206, Svensk Kärnbränslehantering AB.

**Glamheden R, Fredriksson A, Röshoff K, Karlsson J, Hakami H, Christiansson R, 2007.** Rock mechanics Forsmark, Site descriptive modelling Forsmark stage 2.2. SKB R-07-31, Svensk Kärnbränslehantering AB.

**Hakami E, Holmberg J, 2021.** Overcoring of pilot hole in KFM24. Evaluation of the required conditions for future overcoring stress measurements. SKB P-21-12, Svensk Kärnbränslehantering AB.

**Hirashima K, Koga A, 1977.** Determination of stresses in anisotropic elastic medium unaffected by boreholes from measured strains of deformations. In Proc. Int. Symp. On field measurements in rock mechanics (Zurich, 1977), pp. 173-82.

**Klee G, Rummel F, 2004.** Forsmark site investigation. Rock stress measurements with hydraulic fracturing and hydraulic testing of pre-existing fractures in boreholes nos. KFM01A, KFM01B, KFM02A, and KFM04A. Results of in-situ tests. SKB P-04-311, Svensk Kärnbränslehantering AB.

**Leeman E R, 1968.** The determination of the complete state of stress in rock using a single borehole—laboratory and underground measurements. *Int. J. Rock Mech. & Min. Sci.*, 5, pp. 31-56.

**Leeman E R, Hayes D I, 1966.** A technique for determining the complete state of stress in rock using a single borehole. In Proc. 1st Int. Congr. on Rock Mechanics (Lisboa, 1966), Vol. 2, pp. 17-24.

**Merril R H, 1964.** In situ determination of stress by relief techniques. In Proc. Int. Conf. State of stress in the Earth's crust (Santa Monica, 1964), pp. 343-69.

**Ringgaard J, 2007a.** Forsmark site investigation. Mapping of borehole breakouts. Processing of acoustic televiewer data from KFM01A, KFM01B, KFM02A, KFM03A, KFM03B, KFM04A, KFM5A, KFM06A, and KFM07C. SKB P-07-07, Svensk Kärnbränslehantering AB.

**Ringgaard J, 2007b.** Forsmark site investigation. Mapping of borehole breakouts. Processing of acoustic televiewer data from KFM08A, KFM08C, KFM09A, KFM09B, and KFM90B. SKB P-07-166, Svensk Kärnbränslehantering AB.

**Sjöberg J, Klasson H, 2003.** Stress measurements in deep boreholes using the Borre (SSPB) probe. *Int. J. Rock Mech. Min. Sci.*, 40, No. 7-8, pp. 1205-1233.

**Worotnicki G, 1993.** CSIRO triaxial stress measurement cell. In *Comprehensive Rock Engineering*, Vol. 3, (J. Hudson Ed.), Pergamon Press, Oxford, pp. 329-94.

## Appendix 1 – Pilot hole drilling and installations



*Figure A1-1. Pilot 1:1:1 drilled between 562.37-563.09 mbl.*



*Figure A1-2. Pilot 1:1:1 drilled between 562.37-563.09 mbl and overcore sample drilled between 562.49-563.08 mbl.*

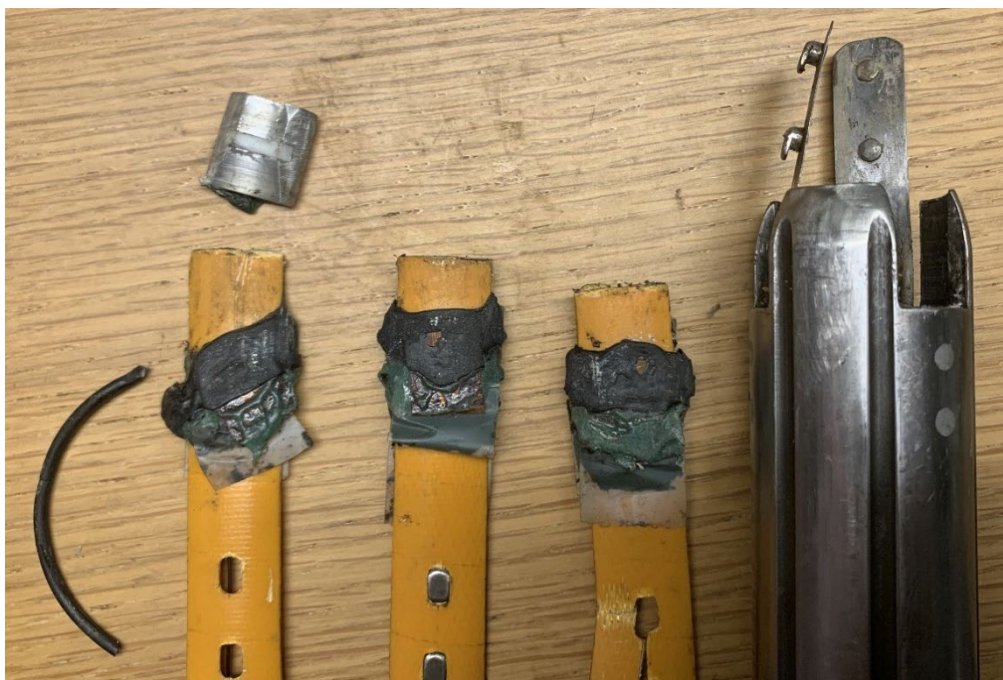


*Figure A1-3. Strain gauge assembly from Test 1:1:1, 562.65 mbl.*



*Figure A1-4. Pilot 1:2:2 drilled between 563.18-563.90 mbl.*



*Figure A1-5. Pilot 1:2:2 drilled between 563.18-563.90 mbl and overcore sample drilled between 563.18-563.81 mbl.*



*Figure A1-6. Photo of overcore sample 1:2:2 taken at position of strain rosette 1.*



*Figure A1-7. Photo of overcore sample 1:2:2 taken at position of strain rosette 2.*



*Figure A1-8. Photo of overcore sample 1:2:2 taken at position of strain rosette 3.*



*Figure A1-9. Strain gauge assembly from Test 1:2:2, 563.32 mbl.*



*Figure A1-10. Pilot 1:3:3 drilled between 563.94-564.69 mbl.*



*Figure A1-11. Pilot 1:3:3 drilled between 563.94-564.69 mbl and overcore sample drilled between 563.97-564.59 mbl.*



*Figure A1-12. Photo of overcore sample 1:3:3 taken at position of strain rosette 1.*



*Figure A1-13. Photo of overcore sample 1:3:3 taken at position of strain rosette 2.*



*Figure A1-14. Photo of overcore sample 1:3:3 taken at position of strain rosette 3.*



*Figure A1-15. Strain gauge assembly from Test 1:3:3, 564.13 mbl.*



*Figure A1-16. Pilot 1:4:4 drilled between 564.86-565.57 mbl.*



*Figure A1-17. Pilot 1:4:4 drilled between 564.86-565.57 mbl and overcore sample drilled between 564.86-565.48 mbl.*



*Figure A1-18. Photo of overcore sample 1:4:4 taken at position of strain rosette 1.*



*Figure A1-19. Photo of overcore sample 1:4:4 taken at position of strain rosette 2.*



*Figure A1-20. Photo of overcore sample 1:4:4 taken at position of strain rosette 3.*

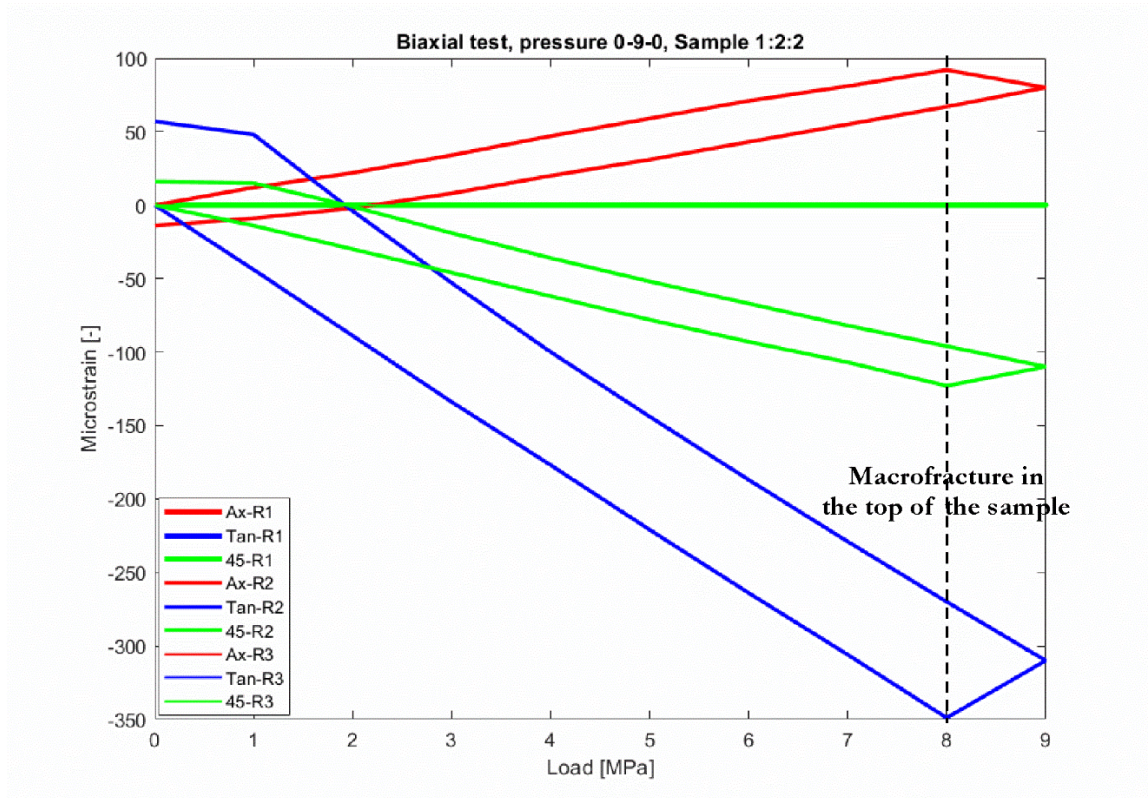


Figure A1-21. Strain gauge assembly from Test 1:4:4, 565.02 mbl.

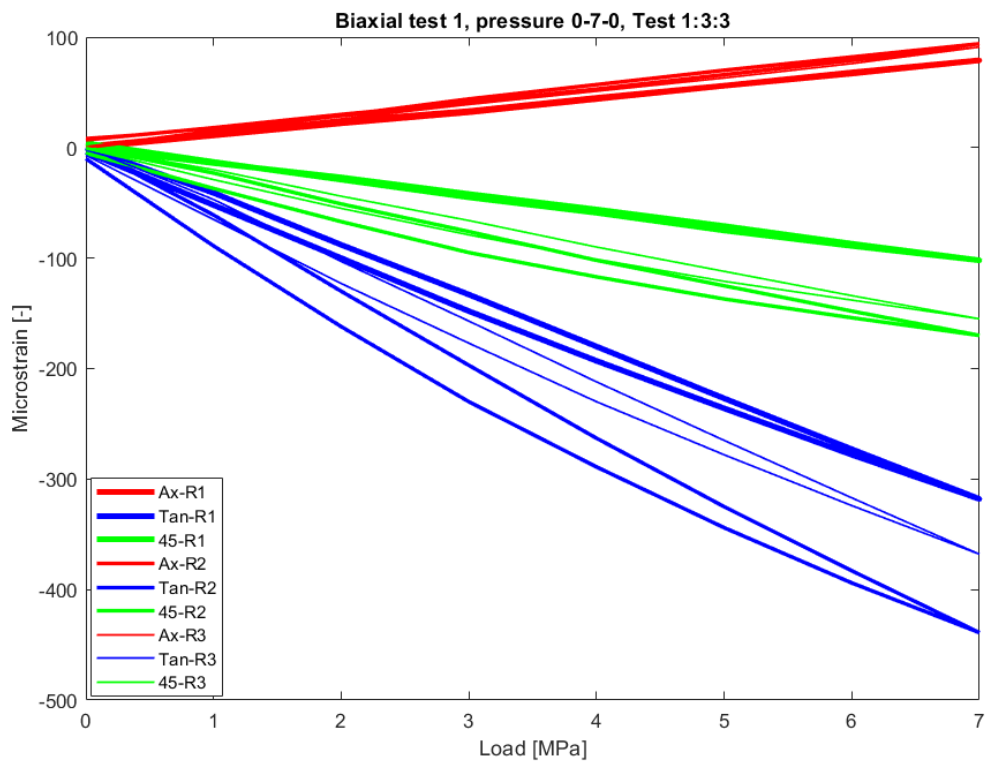


Figure A1-22. Core box after completed drilling in borehole KFM24.

## Appendix 2 – Biaxial test curves



**Figure A2-1.** Biaxial test curve of overcore sample 1:2:2, 563.32 mbl. Only R2 available and core sample fractured during loading.



**Figure A2-2.** Biaxial test curve of overcore sample 1:3:3, 564.13 mbl, first biaxial test.

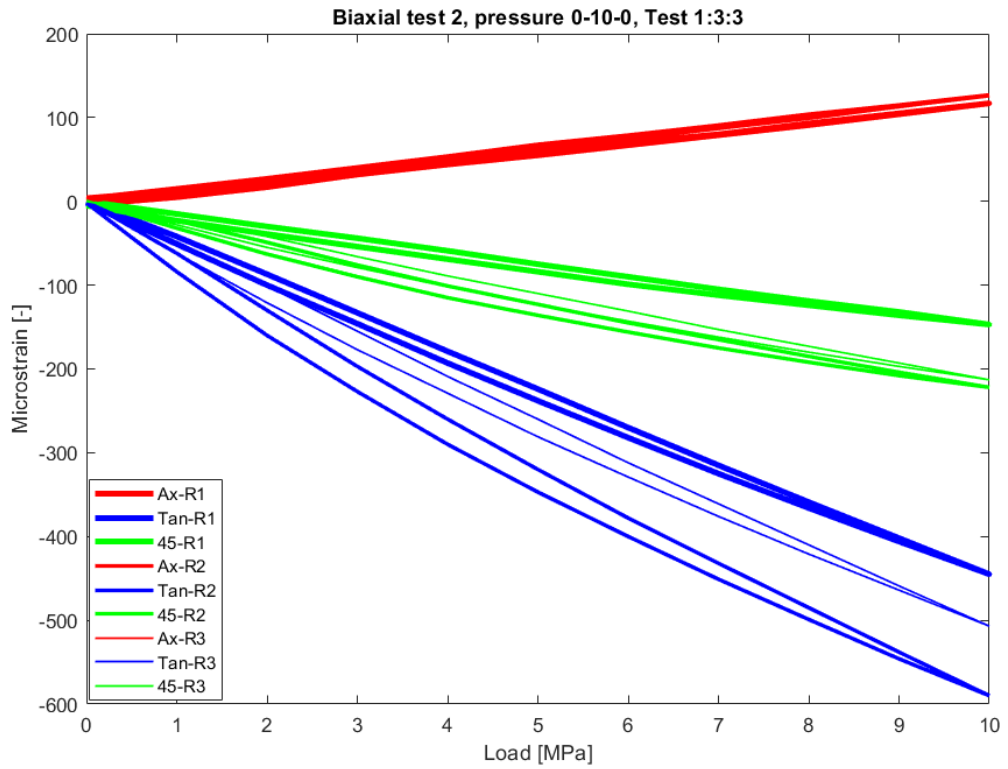


Figure A2-3. Biaxial test curve of overcore sample 1:3:3, 564.13 mbl, second biaxial test.

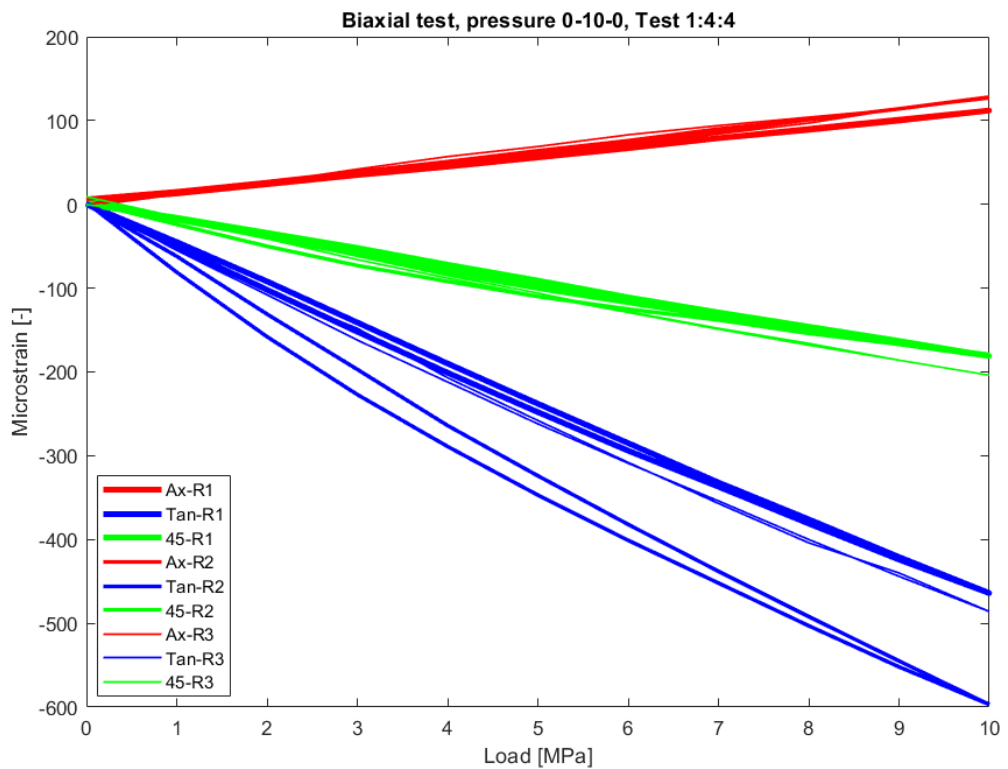


Figure A2-4. Biaxial test curve of overcore sample 1:4:4, 565.02 mbl.

## Appendix 3 – Overcoring strain curves

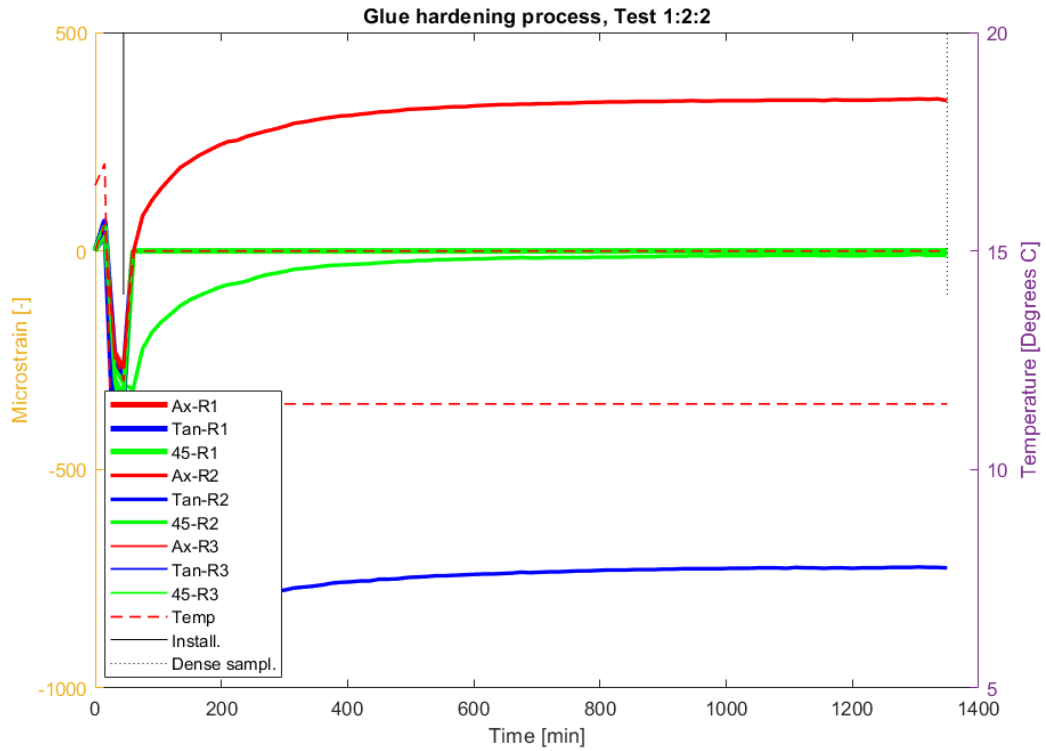


Figure A3-1. Glue hardening curve for Test 1:2:2, 563.32 mbl.

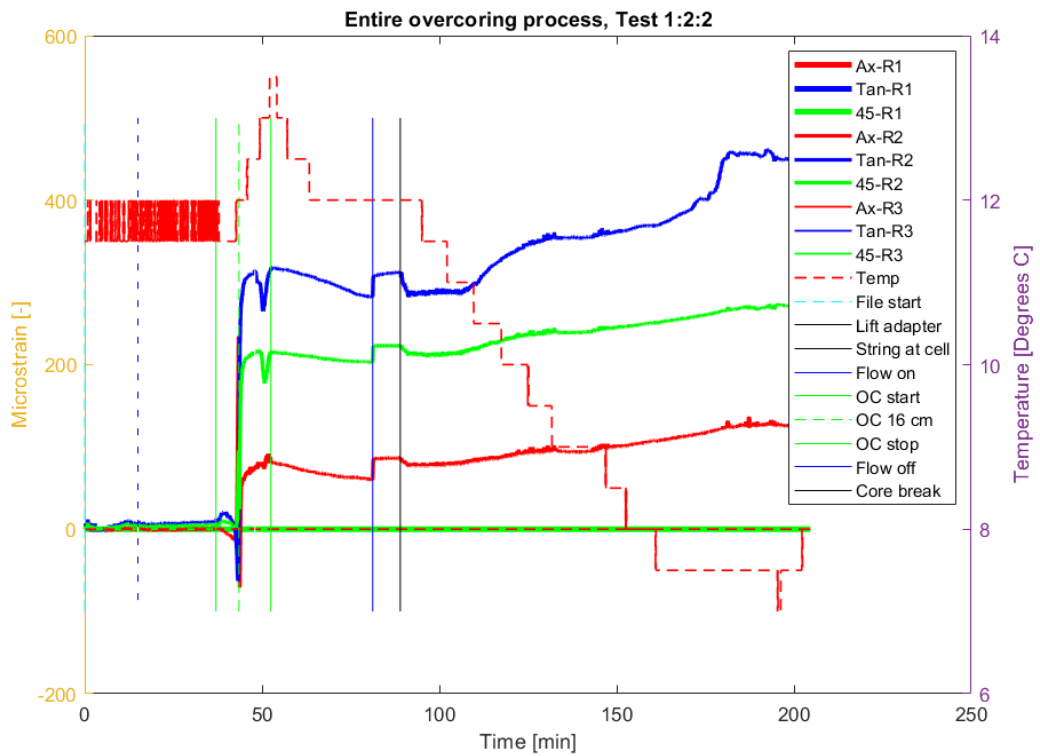


Figure A3-2. Entire overcoring phase for Test 1:2:2, 563.32 mbl.

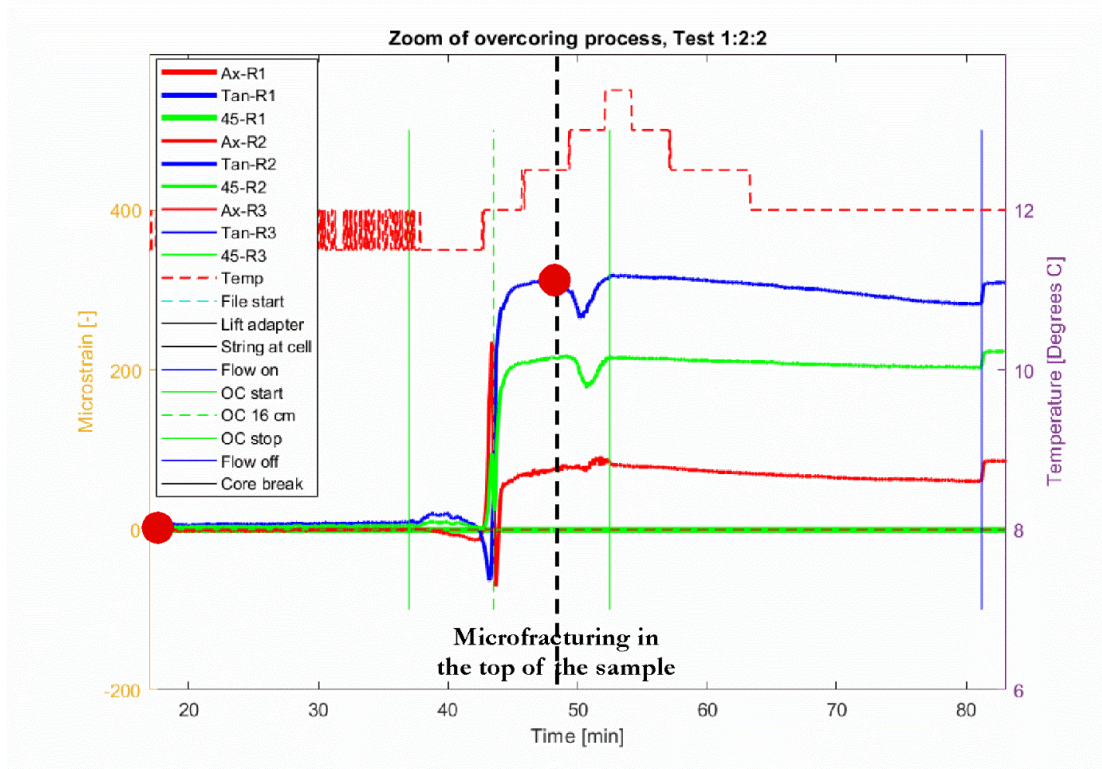


Figure A3-3. Zoom of overcoring phase of Test 1:2:2, 563.32 mbl. Red circles denote strain readings for stress calculation.

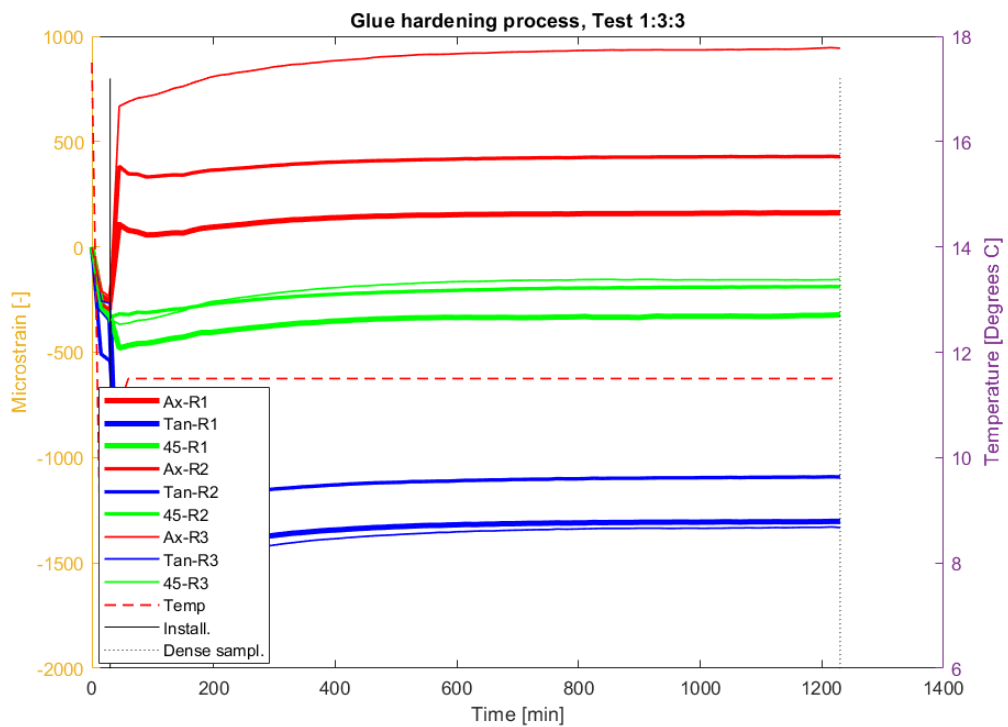


Figure A3-4. Glue hardening curve for Test 1:3:3, 564.13 mbl.

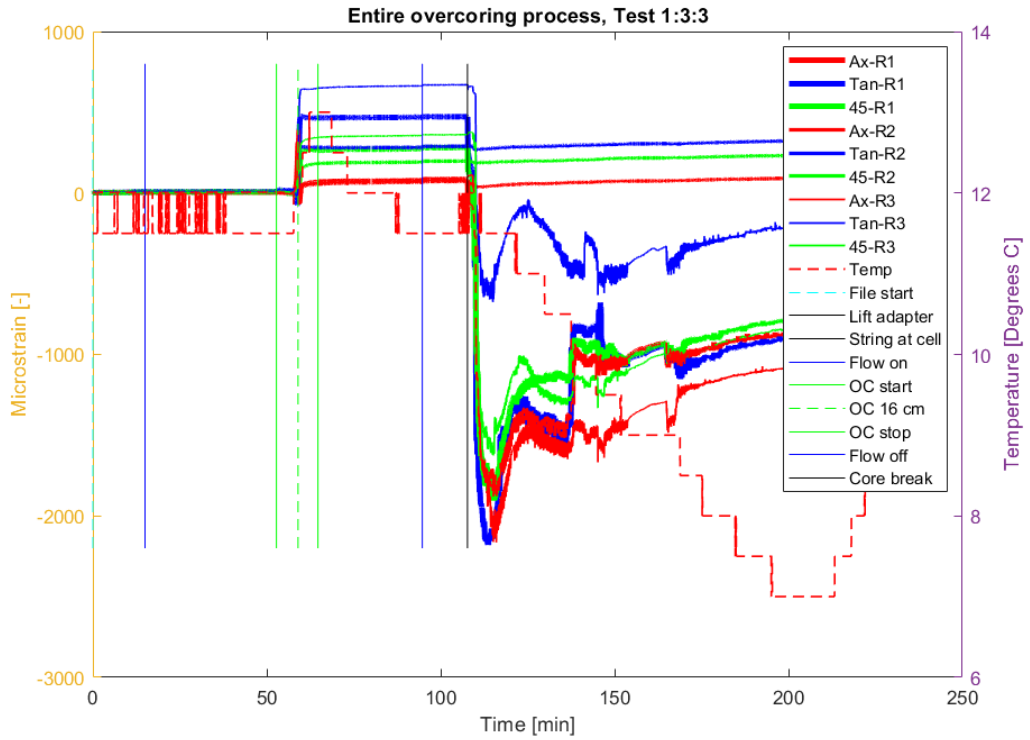


Figure A3-5. Entire overcoring phase for Test 1:3:3, 564.13 mbl.

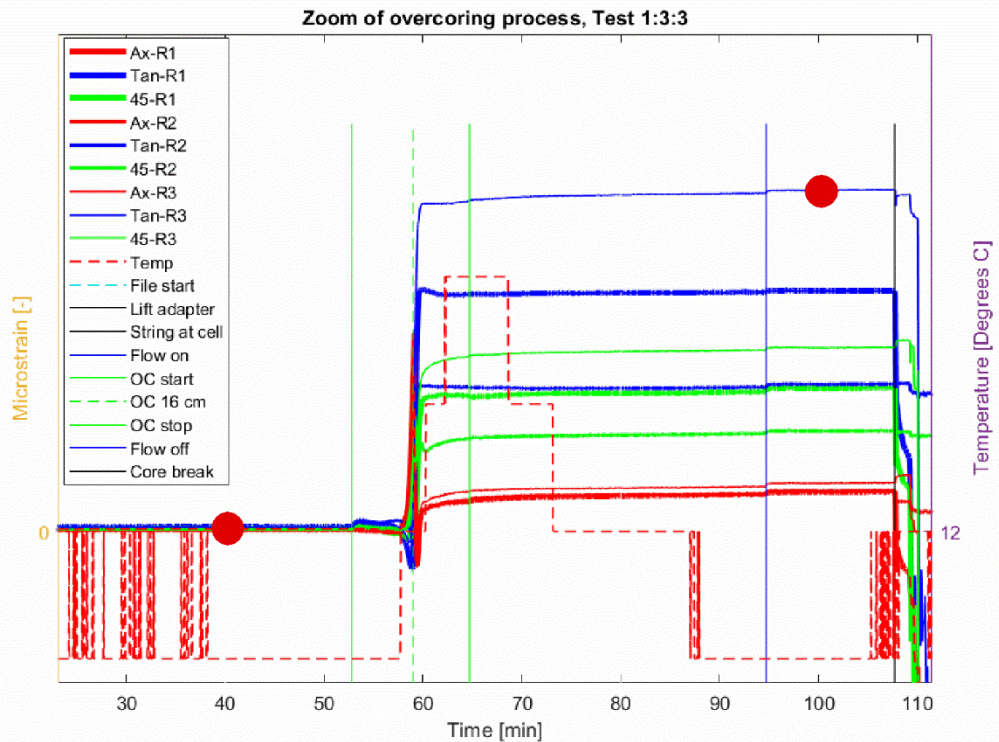


Figure A3-6. Zoom of overcoring phase of Test 1:3:3, 564.13 mbl. Red circles denote strain readings for stress calculation.

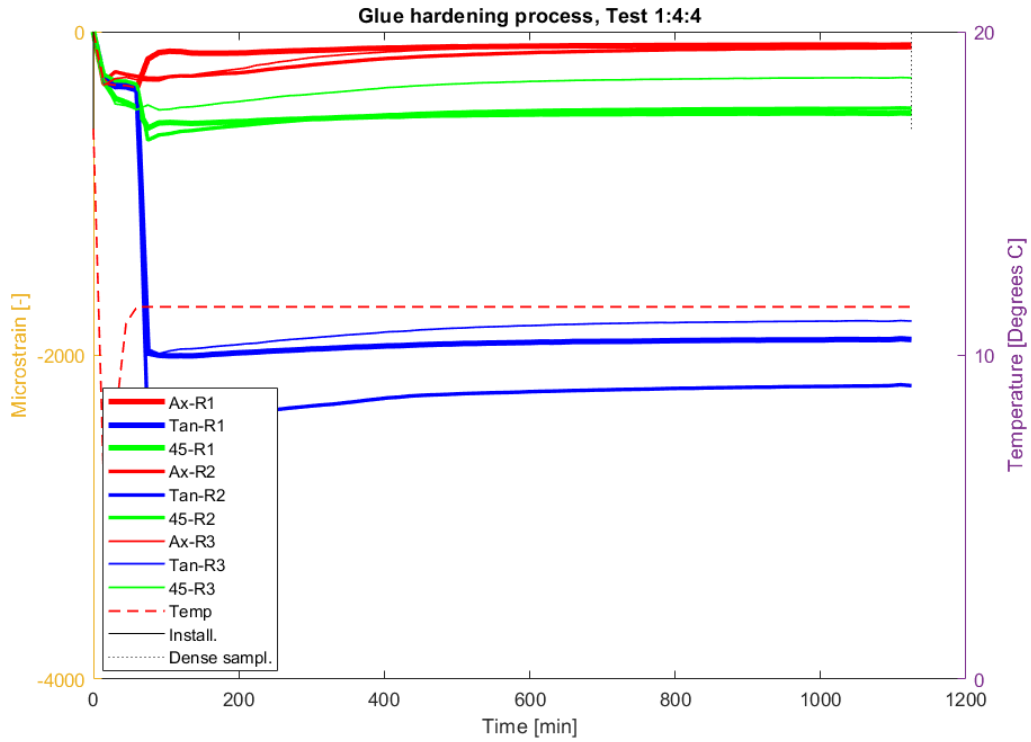


Figure A3-7. Glue hardening curve for Test 1:4:4, 565.02 mbl.

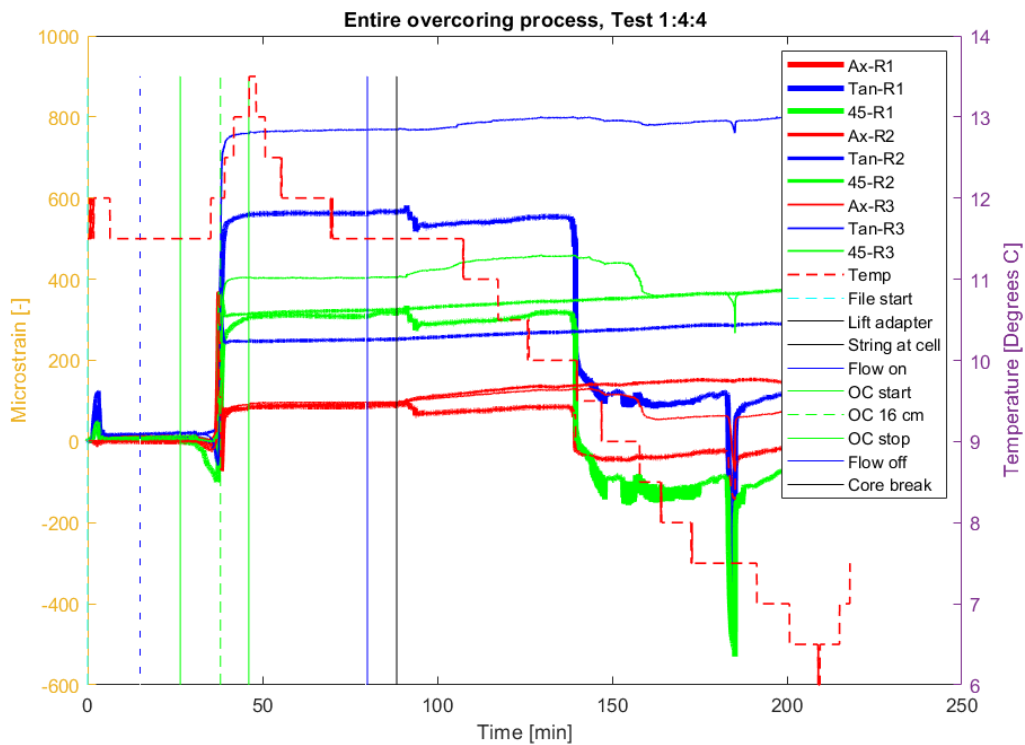
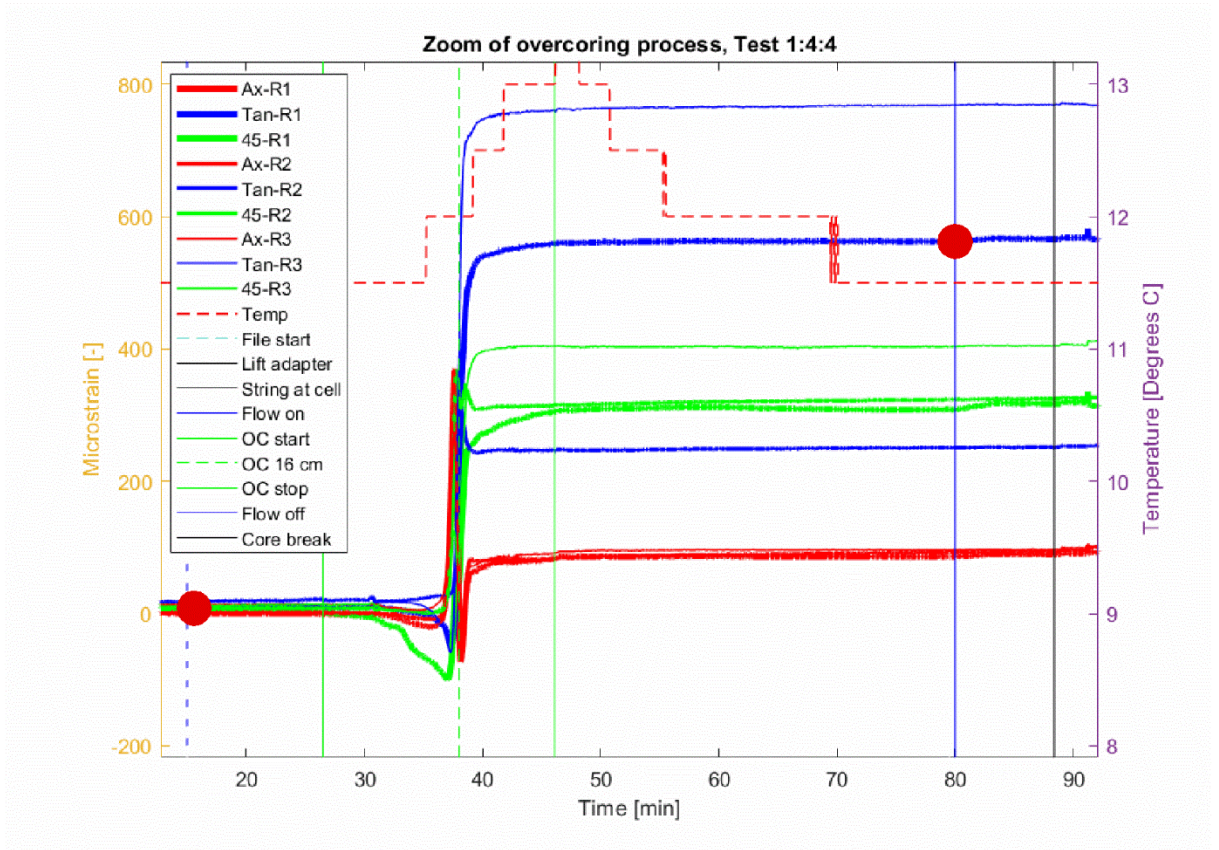


Figure A3-8. Entire overcoring phase for Test 1:4:4, 565.02 mbl.



**Figure A3-9.** Zoom of overcoring phase of Test 1:4:4, 565.02 mbl. Red circles denote strain readings for stress calculation.

## Appendix 4 – Data used for stress calculation

**Table A4-1. Time indications of different phases during overcoring measurements in borehole KFM24.**

Test	Date	Probe installed	Dense sampling	Flushing start	Overcoring start	Overcoring stop	Flushing stop	Core Break	Coring speed	Strain interval used for calculation
1:1:1	250108-09	13:30	08:00	08:18	08:22	08:29	09:02	09:11	8.3 cm/m	-
1:2:2	250115-16	09:55	08:00	08:10	08:35	08:47	09:16	09:24	7.0 cm/m	08:15:00-08:48:00
1:3:3	250122-23	11:48	07:55	08:06	08:50	08:59	09:29	09:42	7.8 cm/m	08:40:00-09:20:00
1:4:4	250202-03	14:25	08:00	08:10	08:34	08:46	09:16	09:29	5.8 cm/m	08:15:00-09:19:30

**Table A4-2. Interpreted strains used for stress calculation in borehole KFM24.**

Test	Depth [mvd]	Compass RT90-RHB70	Ax-1	Tan-1	45-1	Ax-2	Tan-2	45-2	Ax-3	Tan-3	45-3
		[°N]	[μstrain]								
1:1:1	562.65	206	-	-	-	-	-	-	-	-	-
1:2:2	563.32	204	-	-	-	73	307	211	-	-	-
1:3:3	564.13	208	71	463	276	76	283	194	93	661	358
1:4:4	565.02	205	86	551	299	91	233	317	83	750	391

**Table A4-3. Constants used in stress calculations.**

Test	Depth	Direction KFM24	Dip KFM24	E	V
		[°N]	[°]	[GPa]	[-]
1:1:1	562.65	-	-	-	-
1:2:2	563.32	318.5	82.3	71.7	0.22
1:3:3	564.13	318.5	82.3	71.7	0.22
1:4:4	565.02	318.5	82.3	71.7	0.22